INTERNATIONAL JOURNAL OF
COASTAL & OFFSHORE ENGINEERING IJCOE Vol.2/No. 2/Summer 2017 (1-10)

Available online at: http://ijcoe.org/browse.php?a_code=A-10-1-6&sid=1&slc_lang=en

Investigation of Water Circulation and Temperature Effect in Indian Ocean by Perturbation Method

Mojgan Ghazi Mirsaeid[1], Mahdi Mohammad Mahdizadeh[2], Mohammad Reza Bannazadeh[3]

[1] *PhD Student in Hormozgan University; mozhgan_mirsaeid@yahoo.com*
[2*] *Corresponding author: Assistant Prof. of Physical Oceanography, University of Hormozgan; mehdizadeh79@yahoo.com*
[3] *Assistant Prof. of Physical Oceanography, University of Erfan*

ARTICLE INFO

Article History:
Received: 4 Mar. 2017
Accepted: 14 Aug. 2017

Keywords:
perturbation method
heat advection
ocean circulation

ABSTRACT

The tropical Indian Ocean forms the major part of the largest warm pool on Earth, and its interaction with the atmosphere plays an important role in shaping climate on both regional and global scales. Three dimensional temperature fields are calculated analytically for an ocean forced by wind stress and surface heat flux. A basic thermal state involving a balance of lateral and vertical heat diffusion is assumed. An effect of nonlinear heat advection is calculated by a perturbation method. The zero order temperature fields give a rough overall representation of oceanic thermocline. Associated with this field there is a baroclinic eastward flow in the upper part, with a westward return flow below. The interior temperature field to the next order is affected not only by interior heat advection but by heat advection in the Ekman layer, in the up and down welling layers and in the main western boundary current. For solving equations we use perturbation method. All equations are written in spherical coordinate and then compare with results in Cartesian coordinate

1. Introduction

Modeling studies in the Indian Ocean are not as extensive as other oceans in the world. Nevertheless, our current understanding of the dynamics of the North Indian Ocean is largely achieved by numerical models (Shankar, Vinay-Chandran, & Unnikrishnan, 2002). Due to increased interest in Indian Ocean dynamics and its complex circulation compared to other oceans, the study of this ocean has increased in the past decade [1]. The main efforts were made by Scott and McCarey in 2001 and Shankar in 2002.

In 2001, Schott and McCreary explored and interpreted trends in currents at Monsoon's time. In fact, there was a review of the results of observations, theoretical estimates and modeling in the region by others in the context of the reciprocal seasonal flows in southern India, Sri Lanka, and the eastern and central parts of the Arabian Sea [2].

In 2002, Shankar and his colleagues studied the pattern of water flow in the Indian Ocean at the time of Monsoon using a general ocean circulation scheme, and found that seasonal changes in the north of the ocean had regular ups and downs. The flows in the Oman Sea and the Persian Gulf region are not well simulated, and a complete explanation is not provided in the article [3].

In 2009, Frederick and colleagues presented an article on Indian Ocean Fluctuation and climate change, pointing out that the effects of the Indian Ocean on climate change were more than expected. In the article reviews climate phenomena and processes in which the IO is, or appears to be, actively involved. They began with an update of the IO mean circulation and monsoon system. It is followed by reviews of ocean/atmosphere phenomenon at intraseasonal, interannual, and longer time scales. Much of their review addresses the two important types of interannual variability in the IO, El Nin˜o–Southern Oscillation (ENSO) and the recently identified Indian Ocean Dipole (IOD) [4].

In 2014, Muni Krishna and his colleagues studied tropical Indian Ocean surface and subsurface temperature fluctuations in a climate change scenario and its significant impact on Indian monsoon. Tropical Indian Ocean temperature plays a vital on Indian monsoon system and also cyclone genesis. The feature and evolution mechanisms of the tropical Indian Ocean temperature between pre warming and warming period and also during Indian Ocean Dipole

(IOD) events that co-occurred with El Niño are studied using Simple Ocean Data Assimilation (SODA) data set. The southeastern Arabian Sea, Western Arabian Sea and Seychelles Chaogos Thermocline Ridge regions subsurface temperature anomalies are cooled and the southern gyre, south Bay of Bengal, off java regions show warming trend from surface to subsurface [5].

As a mentioned, in most of later experiments, the temptation is to improve oceanic investigation by numerical models by bringing in new effects, such as nonlinear equation of state, etc. The repetitions of experiments over a range of parameter values which give a better insight into the nature of simpler problem, is often neglected. Thus, there seem to be some gaps in our basic theoretical knowledge which need to be filled, by a combination of analytical theory and relatively simple numerical models [12].

The problems studied here involve the calculation of the three dimensional temperature and in a bounded, rectangular ocean on the real earth, forced by a meridionally varying wind stress and surface heat flux. The motion and driving forces are taken to be independent of time. After averaging the equations of motion, the Reynold stresses are defined.

At the solid boundaries, the normal, baroclinic, vertically averaged flow must vanish; hence, boundary layers must form. Actually, this circulation is closed principally through thin upwelling and downwelling layers next to the walls. The zero order temperature fields gives a rough overall representation of oceanic thermocline. The first order calculation of temperature includes not only the advective effects of the interior flow, but equally important effects of thermal advection in the Ekman surface layer and in the barotropic and baroclinic side layers. All equations are written in spherical coordinate and then compare with results in Cartesian coordinate.

2- Data and method

2-1. Basic equations:

Consider a rectangular oceanic basin in spherical coordinate (Fig.1) and then compare results in Cartesian coordinate.

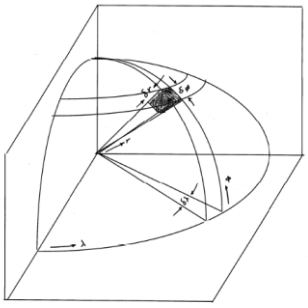

Figure1. Geometry of studied basin in spherical coordinate.

The upper boundary is taken horizontally, r=R, using the so-called rigid–lid, and the horizontal bottom is placed at r=R-H.

At the upper boundary a zonal wind stress and a normal heat flux (counted positive when directed upward) are applied, i.e.:

$$\tau^{\lambda} = -\tau_0 \varphi \sin(k\pi\varphi), \tag{1}$$

$$Q = -Q_0 \cos\frac{\pi}{2}\varphi \tag{2}$$

In Cartesian coordinate $\varphi = \frac{y}{R}$ and in spherical coordinate indicates zonal boundaries in radian. The stress and heat flux are defined as kinematical values (stress divided by density, heat flux divided by heat capacity per unit volume), making their dimensions equal to a velocity square and temperature-time velocity, respectively.

The depth H is assumed small compared to the planetary scale R ($R \gg H$), justifying the hydrostatic balance equation. At the meridional walls, λ=0, 1, it is required that the horizontal velocity and the normal heat flux vanish, while the total velocity and the vertical heat flux vanish at the bottom. At the top the vertical velocity vanishes, while the momentum flux and heat flux are specified according to the boundary conditions (1), (2).

The density variations are assumed small enough to allow the Boussinesq approximation to be valid. In the present formulation, the thermohaline forcing is due entirely to surface heating, but it is possible to include a specified normal flux of salinity S at the surface, giving the effect of evaporation-precipitation processes. If the diffusion coefficient for heat and salt are the same, as is expected to be true when molecular effects are negligible. It is assumed that the turbulent friction and heat diffusion can be described by use of constant eddy coefficients, and that the turbulence is horizontally isotropic, allowing the use of only one coefficient in the horizontal plane. Fluxes due to molecular diffusion are considered negligible relative to the turbulent eddy fluxes.

In accordance with the above description of the problem, the following equations can be written, expressing the horizontal momentum balance, hydrostatic balance, incompressibility, and heat flux divergence balance, respectively:

$$\lambda \text{ direction: } \rho\left(\frac{Du}{Dt} - \frac{uv\tan\varphi}{R} - 2\Omega\sin\varphi v + 2\Omega\cos\varphi w\right) = -\frac{1}{R\cos\varphi}\frac{\partial p}{\partial\lambda} \tag{3}$$

$$\phi \text{ direction: } \rho\left(\frac{Dv}{Dt} + \frac{u^2\tan\varphi}{R} + 2\Omega\sin\varphi u\right) = \frac{1}{R}\frac{\partial p}{\partial\varphi} \tag{4}$$

r direction: $\frac{\partial p}{\partial z} \cong g\alpha T$ (5)

$$\frac{1}{R^2}\frac{\partial}{\partial z}(R^2 w) + \frac{1}{R\cos\varphi}\frac{\partial}{\partial \varphi}(v\cos\varphi) + \frac{1}{R\cos\varphi}\frac{\partial u}{\partial \lambda} = 0 \quad (6)$$

Where $\frac{D}{Dt} = \frac{\partial}{\partial t} + w\frac{\partial}{\partial Z} + \frac{v}{R}\frac{\partial}{\partial \varphi} + \frac{u}{R\cos\varphi}\frac{\partial}{\partial \lambda}$ (7)

The dependent variables are prescribed such that u,v, and w are the velocity components in the λ, ∅, and r directions, P states the pressure, ρ denotes the density, T is the temperature, and g denotes the acceleration of gravity.

After using derivation of stress tensor and Prandtl's Mixing-Length theory and imposing rules of operating on mean time-averaged and some simplifications, the results for momentum balance are:

$$\rho_0\left(\frac{Du}{Dt} - \frac{uv\tan\varphi}{R} - 2\Omega\sin\varphi v - 2\Omega\cos\varphi w\right) = -\frac{1}{R\cos\varphi}\frac{\partial p}{\partial \lambda} + A_H\left(\nabla_H^2 U - \frac{1}{R^2}\left(\frac{\partial U}{\partial \varphi} + \frac{1}{R\cos\varphi}\frac{\partial V}{\partial \lambda}\right)\tan\varphi\right) + A_v\left(\frac{\partial^2 U}{\partial z^2}\right) \quad (8)$$

$$\rho_0\left(\frac{Dv}{Dt} + \frac{u^2\tan\varphi}{R} + 2\Omega\sin\varphi u\right) = \frac{1}{R}\frac{\partial p}{\partial \varphi} + A_H\left(\nabla_H^2 V + \left(\frac{1}{R^2\cos\varphi}\frac{\partial V}{\partial \lambda} + \frac{1}{R}\frac{\partial w}{\partial z}\right)\tan\varphi\right) + A_v\left(\frac{\partial^2 V}{\partial z^2}\right) \quad (9)$$

$$\frac{\partial p}{\partial z} \cong g\alpha T \quad (10)$$

$$\frac{\partial w}{\partial z} + \frac{1}{R\cos\varphi}\frac{\partial v\cos\varphi}{\partial \varphi} + \frac{1}{R\cos\varphi}\frac{\partial u}{\partial \lambda} = 0 \quad (11)$$

And heat balance:

$$\frac{DT}{Dt} = A_H\nabla_H^2 T + A_v\frac{\partial^2 T}{\partial z^2} \quad (12)$$

$$\nabla^2 = \frac{1}{R\cos\varphi}\frac{\partial}{\partial \varphi}\left(\cos\varphi\frac{\partial}{\partial \varphi}\right) + \frac{1}{R^2\cos^2\varphi}\left(\frac{\partial}{\partial \lambda}\right) \quad (13)$$

Boundary conditions become:

$$A_V\frac{\partial U}{\partial z} = \tau_\lambda(\varphi), A_V\frac{\partial T}{\partial z} = -Q(\varphi), \quad \text{at } z = 0 \quad (14\text{-}1)$$

$$\frac{\partial V}{\partial z} = w = 0 \quad \text{at } z = 0 \quad (14\text{-}2)$$

$$U = V = w = \frac{\partial T}{\partial z} = 0 \quad \text{at } z = -H \quad (14\text{-}3)$$

$$U = V = \frac{1}{R\cos\varphi}\frac{\partial T}{\partial \lambda} = 0 \quad \text{at } \lambda = 0,1 \quad (14\text{-}4)$$

$$\frac{1}{R}\frac{\partial U}{\partial \varphi} = V = \frac{1}{R}\frac{\partial T}{\partial \varphi} = 0 \quad \text{at } \varphi = 0,1 \quad (14\text{-}5)$$

2.1. Non-dimensionalization and expansion:

The following transformation to non-dimension variables is introduced:

$$\begin{pmatrix} U \\ V \end{pmatrix} = U_t\begin{pmatrix} U' \\ V' \end{pmatrix}, W = \frac{U_t D}{R}.W' \quad Z = DZ' \quad P = f_0 U_t R.P, \quad T = \Delta T.T' \quad (15)$$

The scale depth D (thermocline depth) is set by balancing the horizontal and vertical heat diffusion, assuming the same typical temperature variation, in both directions. The thermal boundary condition and the thermal wind relation then determines the amplitudes ΔT and U_t. The relations take the form:

$$A_H\frac{\Delta T}{R^2} = A_V\frac{\Delta T}{D^2} \Rightarrow D = \sqrt{\frac{A_V}{A_H}}R \quad (16)$$

$$Q_0 = A_V\frac{\Delta T}{D} \Rightarrow \Delta T = \frac{DQ_0}{A_V} = \frac{RQ_0}{(A_H A_V)^{1/2}} \quad (17)$$

$$\frac{f_0 U_t}{D} = \frac{g\alpha\Delta T}{R} \Rightarrow U_t = \frac{g\alpha R}{A_H f} \quad (18)$$

The non-dimensionalized equations take the corresponding form in spherical coordinate:

$$R_0\left(\frac{U}{COS\varphi}\frac{\partial U}{\partial \lambda} + V\frac{\partial U}{\partial \lambda} + W\frac{\partial U}{\partial Z} - UV\tan\varphi\right) - V\sin\varphi + \frac{DW}{R}\cos\varphi = E\nabla^2 U - E\left(\frac{\partial U}{\partial \varphi} + \frac{1}{COS\varphi}\frac{\partial V}{\partial \lambda}\right)\tan\varphi - \frac{1}{COS\varphi}\frac{\partial P}{\partial \lambda} \quad (19)$$

$$R_0\left(\frac{U}{COS\varphi}\frac{\partial V}{\partial \lambda} + V\frac{\partial V}{\partial \varphi} + W\frac{\partial V}{\partial Z} + U^2\tan\varphi\right) + U\sin\varphi = E(\nabla^2 V + \left(\frac{2}{COS\varphi}\frac{\partial V}{\partial \lambda}\right)\tan\varphi - \frac{\partial P}{\partial \varphi} \quad (20)$$

$$\frac{\partial P}{\partial Z} \cong T \quad (21)$$

$$\frac{\partial W}{\partial Z} + \frac{1}{COS\varphi}\frac{\partial V}{\partial \varphi}COS\varphi + \frac{1}{COS\varphi}\frac{\partial U}{\partial \lambda} = 0 \quad (22)$$

$$R_0\left(\frac{U}{COS\varphi}\frac{\partial T}{\partial \lambda} + V\frac{\partial T}{\partial \varphi} + W\frac{\partial T}{\partial Z}\right) = E(\nabla^2 T) \quad (23)$$

Where the nondimensional numbers appearing in these equations are:

$$R_0 = \frac{U_t}{Rf_0} = \frac{g\alpha}{A_H f_0^2} \quad (24)$$

$$E = \frac{A_H}{f_0 R^2} = \frac{A_V}{f_0 D^2} \quad (25)$$

$$\sigma = \frac{\tau_0 f_0}{g\alpha}\left(\frac{A_H}{A_V}\right)^{1/2} \quad (26)$$

[ratio of wind forcing to thermal forcing]

$$\delta = \frac{D}{H} = \left(\frac{A_V}{A_H}\right)^{1/2}\frac{R}{H} \quad (27)$$

[relative thermocline depth]

The Rossby and Ekman numbers defined above are very small for the real oceans, and it seems natural to try to find a solution in terms of a series developed from these. Using R_0E^{-1} as the expansion parameter, we can write like the following series approximations:

$$T = T_0 + R_0E^{-1}T_1 + (R_0E^{-1})^2T_2 + \cdots, \quad (28)$$

This makes the zero-order thermal balance diffusive. The nonlinear heat advection appears in the first order correction, while the dynamics remain linear.
We can rewrite σ as bellow:

$$\sigma = \frac{\tau_0 f_0}{g\alpha}\left(\frac{A_H}{A_V}\right)^{1/2} = \frac{\tau_0 f_0}{g\alpha}\frac{R}{D} = \frac{\tau f_0 R^2}{A_H f_0 D U_t R} = \frac{\tau}{f_0 D U_t}\frac{A_H}{f_0 R} = \frac{\tau/f_0}{DU_t}E^{-1} \quad (29)$$

$$\sigma^* = \frac{\tau/f_0}{DU_t} \quad (30)$$

The number σ^* gives the ratio of the Ekman wind drift to the thermal wind transport over the thermocline depth. Under the above assumption the zero-order problem is described by:

$$-V_0\sin\varphi + \frac{DW_0}{R}\cos\varphi = E(\nabla^2 U_0 - \left(\frac{\partial V_0}{\partial\varphi} + \frac{1}{COS\varphi}\frac{\partial V_0}{\partial\lambda}\right)\tan\varphi) - \frac{1}{COS\varphi}\frac{\partial P_0}{\partial\lambda} \quad (31)$$

$$U_0\sin\varphi = E(\nabla^2 V_0 + \left(\frac{2}{COS\varphi}\frac{\partial U_0}{\partial\lambda}\right)\tan\varphi) - \frac{\partial P_0}{\partial\varphi} \quad (32)$$

$$\frac{\partial P_0}{\partial Z} \cong T_0 \quad (33)$$

$$\frac{\partial W_0}{\partial Z} + \frac{1}{COS\varphi}\frac{\partial(V_0\cos\varphi)}{\partial\varphi} + \frac{1}{COS\varphi}\frac{\partial U_0}{\partial\lambda} = 0 \quad (34)$$

$$\nabla^2 T_0 \cong 0 \quad (35)$$

With the nonhomogeneous boundary conditions:

$$E\frac{\partial U_0}{\partial Z} = \sigma^*\varphi\sin\pi\varphi \quad (36)$$

$$\frac{\partial T_0}{\partial Z} = \cos\frac{\pi\varphi}{2} \quad (37)$$

Both prescribed at z=0, and with homogeneous boundary conditions:

$$U_0 = V_0 = W_0 = \frac{\partial T_0}{\partial Z} = 0 \quad \text{at } z = -\frac{H}{D} = -\frac{1}{\delta} \quad (38)$$

$$U_0 = V_0 = \frac{1}{RCOS\varphi}\frac{\partial T_0}{\partial\lambda} = 0 \quad \text{at } \lambda = 0,1 \quad (39)$$

$$\frac{1}{R}\frac{\partial U_0}{\partial\varphi} = V_0 = \frac{1}{R}\frac{\partial T_0}{\partial\varphi} = 0 \quad \text{at } \varphi = 0,1 \quad (40)$$

$$W_0 = \frac{\partial V_0}{\partial Z} = 0 \quad \text{at } z = 0 \quad (41)$$

3. Results

3.1. The zero order solution for temperature

The solution to the heat diffusion equation with the top boundary conditions is independent of λ. We can write:

$$\frac{\partial^2 T_0}{\partial Z^2} + \frac{1}{\cos\phi}\frac{\partial}{\partial\phi}(\cos\phi\frac{\partial T_0}{\partial\varphi}) = 0 \quad (42)$$

With boundary condition:

$$\frac{\partial T_0}{\partial Z} = \cos\frac{\pi}{2}\varphi \quad \text{at } Z = 0$$
$$\frac{\partial T_0}{\partial\varphi} = 0 \quad \text{at } \varphi = 0,1 \quad (43)$$
$$\frac{\partial T_0}{\partial Z} = 0 \quad \text{at } z = -\frac{H}{D} = -\frac{1}{\delta}$$

The solution becomes:

$$T_0 = \cos\frac{\pi\phi}{2}\cdot\frac{\cosh\frac{\pi}{2}(Z+\frac{1}{\delta})}{\frac{\pi}{2}\sinh(\frac{\pi}{2\delta})} + \sum_{n=1}^{\infty}\sum_{m\neq 1}^{\infty} c_0(n,m)\cos\left(\pi - \frac{1}{2}\right)\pi\varphi\cos(m-1)\pi\delta Z \quad (44)$$

The first term in the solution is because of, horizontally the solution varies as $\cos\frac{\pi\phi}{2}$; hence the vertical variation is of the form $Ae^{\pi z/2} + Be^{-\pi z/2}$; second term is a summation which is due to the assumed spheroid of the earth's surface vs. $c_0(n,m)$ are obtained by substituting (16) into (42), Fourier decomposing the equation in the ϕ and Z directions

and solving the resultant relations for $c_0(n,m)$. The T_0 solution is depicted in Fig. 2.

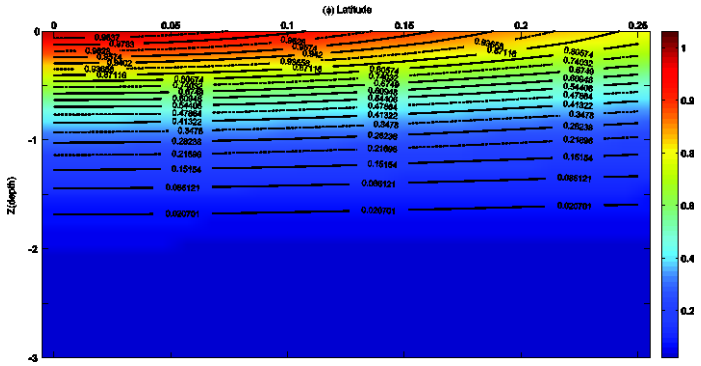

Figure 2- The T_0 field in a meridional section (solid and dash lines indicate spherical and ß plane coordinate results).

3.2. The first-order temperature:

The first order correction T_1 to the temperature field satisfies below equation.

$$\nabla^2 T_1 = \frac{u_0}{cos\emptyset}\frac{\partial T_0}{\partial \lambda} + V_0\frac{\partial T_0}{\partial \emptyset} + w_0\frac{\partial T_0}{\partial z} \tag{45}$$

Since T_0 is independent of λ this equation takes on the simpler form:

$$\frac{\partial^2 T_1}{\partial Z^2} + \frac{1}{\cos\phi}\frac{\partial}{\partial\phi}\left(\cos\phi\frac{\partial T_1}{\partial\varphi}\right) + \frac{1}{\cos^2\emptyset}\frac{\partial^2 T_1}{\partial\lambda^2} = V_0\frac{\partial T_0}{\partial\varphi} + W_0\frac{\partial T_0}{\partial z} \tag{46}$$

With the right-hand side a function of z and ϕ only. The boundary conditions are homogeneous, i.e.,

$$\frac{\partial T_1}{\partial Z} = 0 \qquad \text{at } z = 0 \text{ and } z = -\frac{1}{\delta}$$
$$\frac{\partial T_1}{\partial \lambda} = 0 \qquad \text{at } \lambda = 0 \text{ and } \lambda = 1$$
$$\frac{\partial T_1}{\partial \varphi} = 0 \qquad \text{at } \varphi = 0,1$$

For better understanding, we suppose the total problem as the sum of four sub-problems:

$$T_1 = T_{11} + T_{12} + T_{13} + T_{14} \tag{47}$$

$$1.\ \nabla^2 T_{11} = V_0\frac{\partial T_0}{\partial\emptyset} + w_0\frac{\partial T_0}{\partial z} \tag{48}$$

And all boundary conditions are homogeneous. This solution reflects the effect of the interior solution.

$$2.\ \nabla^2 T_{12} = 0 \tag{49}$$

$$\frac{\partial T_1}{\partial z} = \sigma^*\frac{\emptyset sink\pi\emptyset}{sin\emptyset}\frac{\partial T_0}{\partial\emptyset} \quad at \quad z = 0 \tag{50}$$

With the boundary condition (50) and other homogeneous conditions, T_{12} indicates the effect of the Ekman layer advection.

$$3.\ \nabla^2 T_{13} = 0 \tag{51}$$

With the boundary condition

$$\frac{\partial T_{13}}{\partial\lambda} = \sigma^*\delta\sum\sum B(n,m)\cos\left(n - \frac{1}{2}\right)\pi\emptyset\cos(m - 1)\pi\delta z \quad \text{at} \quad \lambda = 0 \tag{52}$$

and other conditions are homogeneous. T_{13} reflects the effect of western boundary current advection.

$$4.\ \nabla^2 T_{14} = 0 \tag{53}$$

With the condition:

$$\frac{\partial T_{14}}{\partial\lambda} = \sum\sum D(n,m)\cos\left(n - \frac{1}{2}\right)\pi\emptyset\cos(m - 1)\pi\delta z \quad \text{at } \lambda = 0 \text{ and } \lambda = 1 \tag{54}$$

and other conditions are homogeneous. T_{14} indicates the effect of baroclinic upwelling and downwelling near $\lambda = 0$ and 1 .

3.2.1. Interior Solution

The interior advection solution T_{11} has forcing which is independent of λ and the governing equation can be written as:

$$\frac{\partial^2 T_{11}}{\partial Z^2} + \frac{1}{\cos\phi}\frac{\partial}{\partial\phi}\left(\cos\phi\frac{\partial T_{11}}{\partial\varphi}\right) = V_0\frac{\partial T_0}{\partial\varphi} + W_0\frac{\partial T_0}{\partial z} \tag{55}$$

Where T_0, V_0 and $W_0$are define as equation (16) and (56) respectively.

$$V_0 = \sigma^*\left(\frac{1}{cos\varphi}\left(sink\pi\varphi + k\pi\varphi\ cosk\pi\varphi - \frac{\varphi sink\pi\varphi}{cos^2\varphi sin\varphi}\right)\right)\delta$$
$$W_0 = \sigma^*\left(\frac{1}{sin\varphi}\left(sink\pi\varphi + k\pi\varphi\ cosk\pi\varphi - \frac{\varphi sink\pi\varphi}{sin^2\varphi cos\varphi}\right)\right)(1+\delta z)\delta \tag{56}$$

The solution to equation (55) is:

$$T_{11} = \sigma^{*}\delta \sum_{n=1}^{\infty}\sum_{m=1}^{\infty} c_{11}(n,m)\cos\left(n - \frac{1}{2}\right)\pi\varphi\cos[(m-1)\pi\delta Z] \quad (57)$$

By substituting equation (57) into equation (55), Fourier decomposing in the $\emptyset$ and Z directions and solving the resulting equations, $c_{11}(n,m)$ are obtained. According to equation (55), the nonlinear interior temperature advection to first order is due to the meridional and vertical (barotropic) motions. Fig3a indicates the meridional temperature advection and Fig 3b shows the vertical temperature advection in the interior, i.e. the right hand side of equation (55).

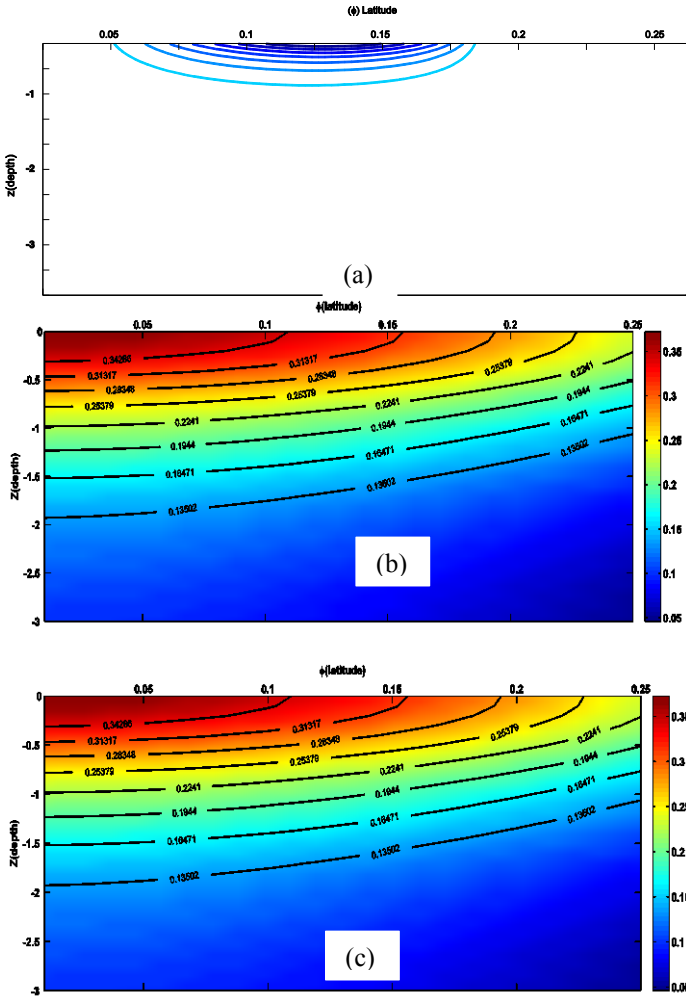

Figure 3. The interior forcing functions of T_{11} field in a meridional section: (a) Meridional advection, (b) Vertical advection,(c) total (meridional plus vertical advection)

3-2-2-Ekman advection

Next consider the Ekman transport induced temperature T_{12}. The non-homogeneous boundary condition at Z=0 is independent of λ; the governing equation is as follows:

$$\frac{\partial^2 T_{12}}{\partial Z^2} + \frac{1}{\cos\phi}\frac{\partial}{\partial\phi}\left(\cos\phi\frac{\partial T_{12}}{\partial\varphi}\right) = 0 \quad (58)$$

With the homogeneous and below boundary conditions:

$$\frac{\partial T_{12}}{\partial Z} = \sigma^{*}\sum_{\text{at } Z=0} A_n\cos\left(n-\frac{1}{2}\right)\pi\emptyset \quad (59)$$

The solution to equation (50) is:

$$T_{12} = \sigma^{*}\left(\frac{\delta z^2}{2} + z\right)\sum A_n\cos\left(n-\frac{1}{2}\right)\pi\emptyset + \sigma^{*}\sum\sum c_{12}(n,m)\cos\left(n-\frac{1}{2}\right)\pi\emptyset\cos(m-1)\pi\delta z \quad (60)$$

The coefficients $c_{12}(n,m)$ are obtained by substituting equation (60) into (58), by invoking the orthogonally property of $\cos\left(n-\frac{1}{2}\right)\pi\emptyset$ and $\cos(m-1)\pi\delta z$ and by solving the resulting equations for $c_{12}(n,m)$.

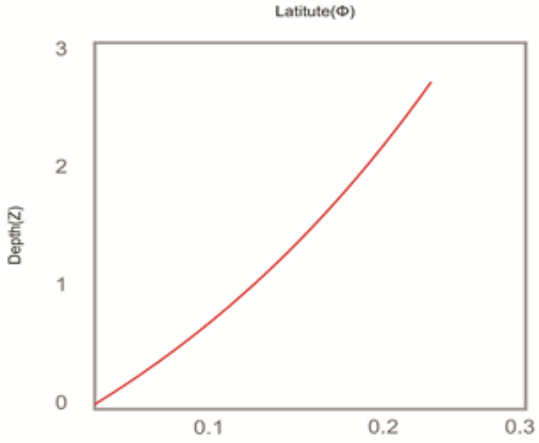

Figure4. Forcing function at the top Ekman layer.

The Ekman layer will transport warm water. Since T_0 decreases as $\emptyset$ increases, in the tropical gyre $V_E\frac{\partial T_{12}}{\partial\emptyset} < 0$ and there is an upward advection of warm water as well as a diffusion of heat down from the Ekman layer. So as is shown by fig. 4, Forcing function at the top Ekman layer is positive at low latitudes. As seen from Fig. 5, at low latitudes, the Ekman layer is a source of heat ($T_{12} > 0$) .

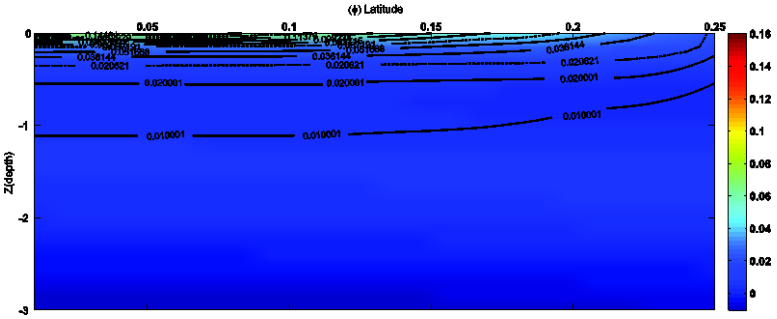

Figure 5. The T2 field in a meridional section (solid and dash lines indicate spherical and ß plane coordinate results).

3-2-3- western boundary current

Now consider the western boundary current advection solution, T_{13}. The governing equation defining T_{13} is as follows:

$$\frac{\partial^2 T_{13}}{\partial Z^2}+\frac{1}{\cos\phi}\frac{\partial}{\partial\phi}\left(\cos\phi\frac{\partial T_{13}}{\partial\varphi}\right)+\frac{1}{\cos^2\varphi}\frac{\partial^2 T_{13}}{\partial\lambda^2}=0 \qquad (61)$$

With the homogeneous and below boundary conditions:

$$\frac{\partial T_{13}}{\partial\lambda}=\delta\sum_{n=1}^{\infty}\sum_{m=1}^{\infty}\sigma^{*}B(n,m)\cos\left(n-\frac{1}{2}\right)\pi\varphi\cos(m-1)\pi\delta z \qquad \text{at } \lambda=0$$

The solution to equation (61) is:

$$T_{13}=\sigma^{*}\delta\left(\lambda-\frac{\lambda^2}{2}\right)\sum_{n=1}^{\infty}\sum_{m=1}^{\infty}B(n,m)\cos\left(n-\frac{1}{2}\right)\pi\varphi\cos(m-1)\pi\delta z+\sigma^{*}\delta\sum_{n=1}^{\infty}\sum_{m=1}^{\infty}\sum_{n=1}^{\infty}C_{13}(n,m,k)\cos\left(n-\frac{1}{2}\right)\pi\varphi\cos(m-1)\pi\delta z\cos(k-1)\pi\lambda \qquad (62)$$

Where $C_{13}(n,m,k)$ and $B(n,m)$ are obtained by substituting equation (62) into equation (60), Fourier decomposing in the Ø and Z directions and solving the resulting equations for them.

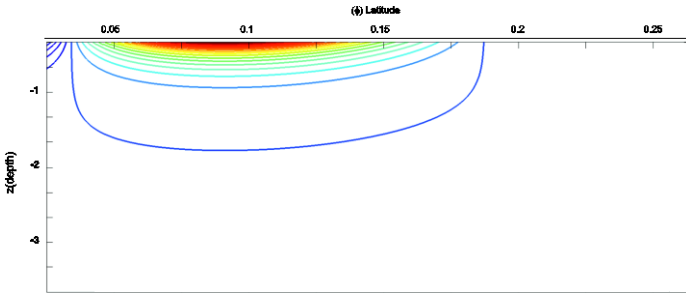

Figure6. The forcing function at the western side.

We have $\frac{\partial T_{13}}{\partial\lambda}<0$ at the edge of boundary current. The heat advected to higher latitudes by the boundary current diffuse into the interior (Fig. 6). The effect in the tropical gyre is small, since $\frac{\partial T_{13}}{\partial\lambda}$ is small and the transport is also small. $T_{13}$is positive everywhere so the net effect is warming of the water everywhere, as seen in Fig. 7a,b,c.

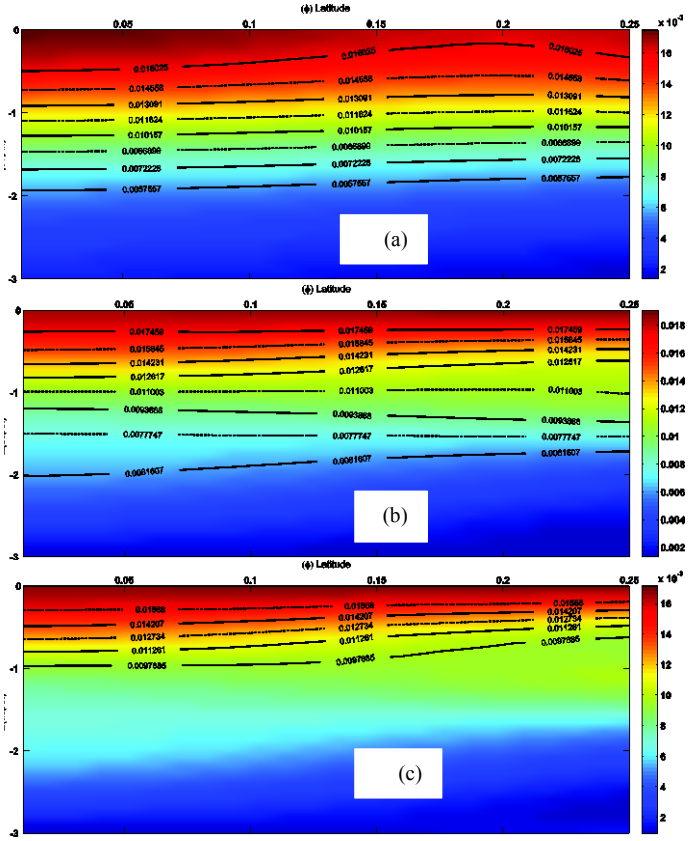

Figure7. T_{13} field in a meridional section. (a) λ=0, (b) λ=0.5, (c) λ=1
(solid and dash lines indicate spherical and ß plane coordinate results).

3-2-4- upwelling and downwelling

The coastal upwelling induces the solutionT_{14} .The equation governing T_{14} is:

$$\frac{\partial^2 T_{14}}{\partial Z^2}+\frac{1}{\cos\phi}\frac{\partial}{\partial\phi}\left(\cos\phi\frac{\partial T_{14}}{\partial\varphi}\right)+\frac{1}{\cos^2\varphi}\frac{\partial^2 T_{14}}{\partial\lambda^2}=0 \qquad (63)$$

With the homogenous and below boundary conditions:

$$\frac{\partial T_{14}}{\partial\lambda}=\sum_{n=1}^{\infty}\sum_{m=1}^{\infty}D(n,m)\cos\left(n-\frac{1}{2}\right)\pi\varphi\cos\left(m-\frac{1}{2}\right)\pi\delta z \qquad \text{at } \lambda=0,1 \qquad (64)$$

The solution to equation (63) is:

$$T_{14}=\lambda\sum_{n=1}^{\infty}\sum_{m=1}^{\infty}D(n,m)\cos\left(n-\frac{1}{2}\right)\pi\varphi\cos\left(m-\frac{1}{2}\right)\pi\delta z+\sum_{n=1}^{\infty}\sum_{m=1}^{\infty}\sum_{n=1}^{\infty}C_{14}(n,m,k)\cos\left(n-\frac{1}{2}\right)\pi\varphi\cos\left(m-\frac{1}{2}\right)\pi\delta z\cos(k-1)\pi\lambda \qquad (65)$$

Where the values of $D(n,m)$ and $C_{14}(n,m,k)$ are obtained by substituting equation (65) into equation (63), using the orthogonally property of $\cos\left(n-\frac{1}{2}\right)\pi\varphi$ and $\cos\left(m-\frac{1}{2}\right)\pi\delta z$ and solving the resulting equation for $C_{14}(n,m,k)$.

The baroclinic upwelling and downwelling next to the meridional boundaries produce a positive value of $\frac{\partial T}{\partial \lambda}$ at the western and eastern sides (Fig. 8), i.e., cooling effects at the western boundary and heating at the eastern boundary. We find a diffusion heat from east to west.

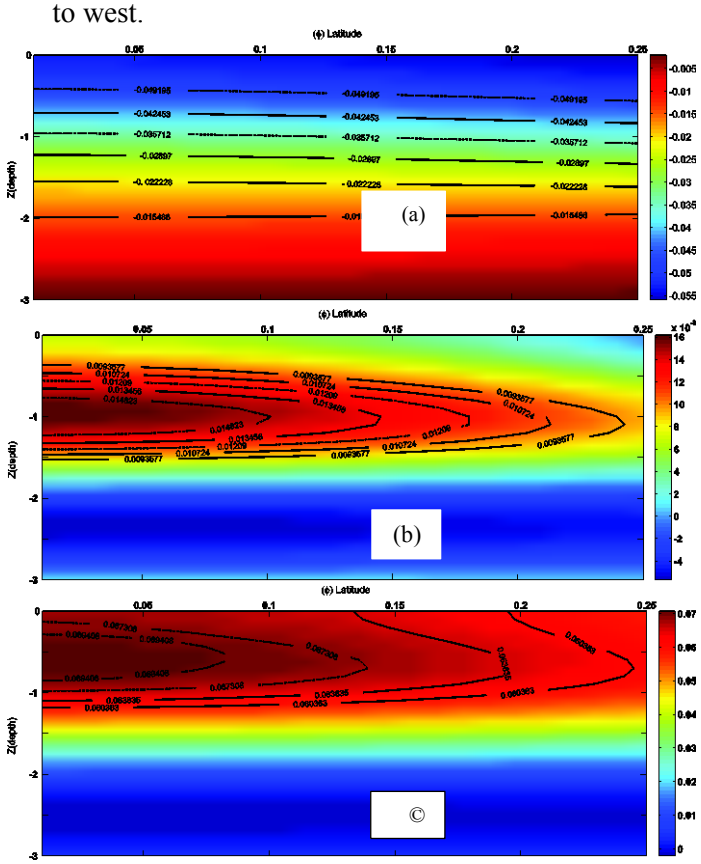

Figure8. T_{14} field in a meridional section. (a) λ=0, (b) λ=0.5, (c) λ=1
(solid and dash lines indicate spherical and ß plane coordinate results).

3.3. Comparing Results in Cartesian and Spherical Coordinate

From the zero order solution, we display the temperatures field which is produced by diffusive balance. Heating over the ocean surface diffuses throughout ocean. The zero order temperature field has a smooth meridional variation, with the isotherms starting out horizontally from the equator and rising to the surface exponentially, as shown in Fig.2. The spherical-system generally shows warmer temperatures and a deeper thermocline than the ß-plane system and there is approximately 10% difference between the two cases.

The first order temperature field has been divided into four sub-problems as described in the former section. The nonlinear interior temperature advection to first order is due to the barotropic velocity. Fig.3a indicates the meridional temperature advection forcing function and Fig. 3b shows the vertical temperature advection forcing function in the interior. Since the vertical advection is stronger than meridional advection, the major effect will be due to vertical advection. Fig.3c gives the total interior advective forcing.

Considering equation (46) for T_{11}, one can see that a positive advection term corresponds to a heat sink in the first order calculation and a strong, unbalanced interior heat sink at low latitudes. The difference between the ß-plane and the spherical-system in the vertical advection is reasonable at low latitudes (5%). In the meridional advection, the difference will be between 20% and 50%. The spherical-system shows less cooling than the ß-plane system result.

The Ekman layer will transport warm water. As is shown by Fig. 4, the corrected boundary condition is positive. As seen from Fig. 5, the Ekman layer is a source of Heat. The difference between the ß-plane and the spherical-system is about 20%.

The western boundary current advection is barotropic. As shown in Fig. 6, the effect in the tropical gyre is negative and small, as $\frac{\partial T_3}{\partial \lambda}$ is small, the transport is less. T_{13} is positive everywhere so the net effect is a warming of the water everywhere, as seen in Figs. 7a, 7b and 7c. There is about 10% to 25% difference, with the spherical-system showing warmer temperatures.

In Fig 8, isotherms in western side indicate cooling but for eastern side there is an opposite sign, which indicates warming there.There is a small difference between the ß-plane and spherical system. It is about 5% zonally, which seems reasonable since in the east-west direction, the β effect is not important.

If we add the three wind induced temperature corrections together (T_{11}+T_{12}+T_{13}), At low latitudes there is a cooling due to interior advection. Also, there is a difference between the ß-plane system and sp-system of about 10% at low latitudes (see Fig.9).

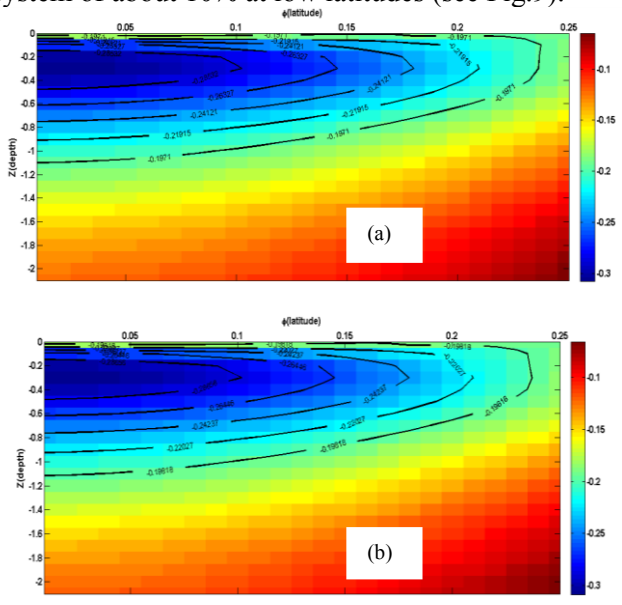

Figure9. the solution to problems T1+T2+T3 for (a) λ=0, (b)λ=1

If we add the baroclinic upwelling and downwelling to the first three results we will have an additional cooling along the western side. This is seen in Fig. 10.

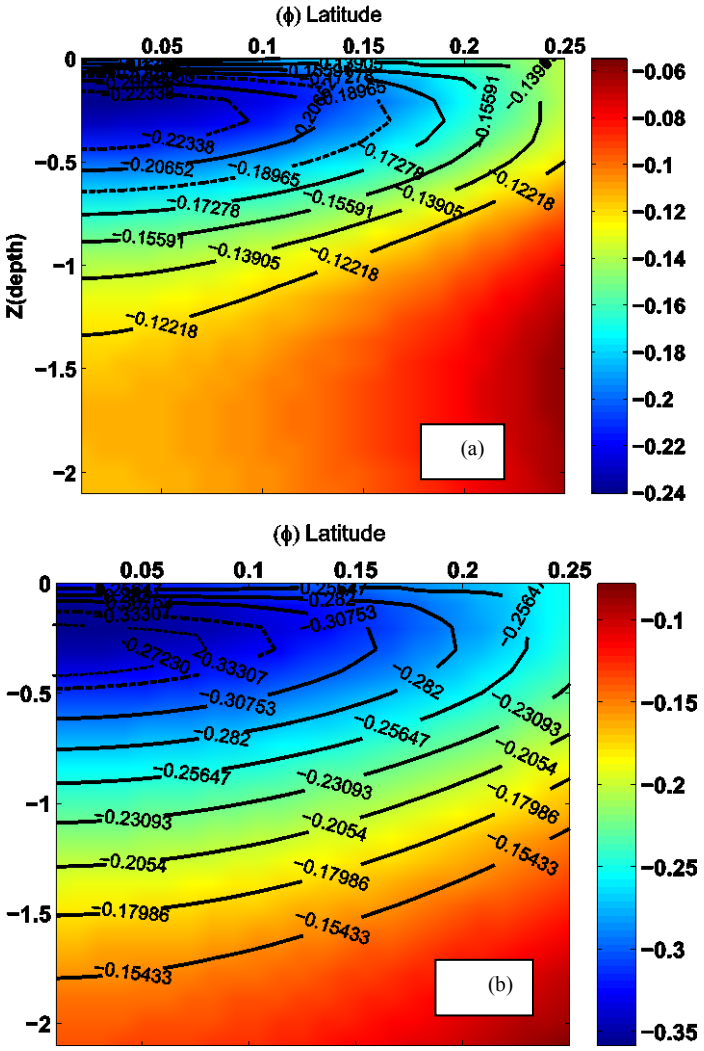

Figure10- the solution to problems $T_1+T_2+T_3+T_4$ for (a) λ=0, (b)λ=1

The total field, $T_0+T_1R_0E^{-1}$, shown in Fig. 11, is reasonable. the isotherms are shallow at the equator and reach a maximum depth at mid-latitude and then rise to surface exponentially.

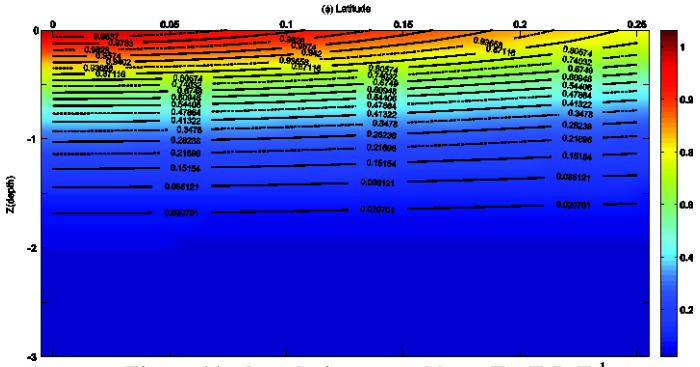

Figure 11- the solution to problems $T_0+T_1R_0E^{-1}$

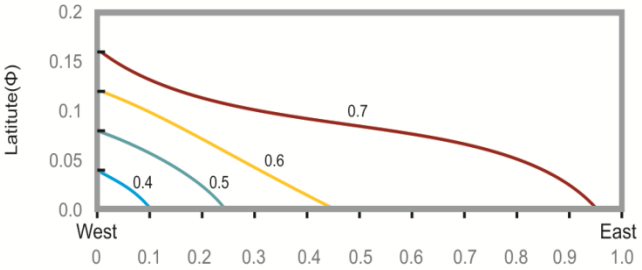

Figure12. total solution $T_0+T_1R_0E^{-1}$ at z=0

Fig. 12 shows the surface temperature field, $T_0+T_1R_0E^{-1}$. In the tropical region, the eastern surface water is warmer than the western surface water, since in the tropical region there is a downward slope of the isotherms to the north, we will have a westward baroclinic current in the upper layer at low-latitudes.

Summary and Conclusions:

Now let us summarize the results of this paper. The zero order temperature field gives on overall representation of the ocean thermocline. Associated with this field there is a baroclinic eastward flow in the upper layer with a weak westward return flow below. This circulation is closed in the upwelling and down welling layers at the western and eastern sides, respectively. The first order correction, T1, is divided into four temperature fields. The nonlinear interior advection is due to the meridional and vertical advection and produces cooling everywhere. The Ekman layer will transport warm water and there is an upward advection of warm water as well as a diffusion of heat down from the Ekman. The Ekman layer is a source of heat. After considering the western boundary current advection solution, it is find the effect in the tropical gyre is small, since $\frac{\partial T_{13}}{\partial \lambda}$ is small and the transport is also small. Since T_{13} is positive everywhere so the net effect is warming of the water everywhere.

The baroclinic upwelling and downwelling next to the meridional boundaries produce a positive value of $\frac{\partial T}{\partial \lambda}$ at the western and eastern sides. Cooling effects at the western boundary and heating at the eastern boundary. We find a diffusion heat from east to west.

If we add the first three temperature fields together, the net effect is a cooling of surface water near the northern boundary due to the Ekman advection. If we superpose the effect of upwelling, it will add an additional cooling along the western side and additional warming along the eastern side.

The total temperature field $(T_0 + T_1RE^{-1})$ gives a result which seems reasonable. The thermocline is shallow and concentrated at the equator. Isotherms reach a maximum depth at mid-latitudes.

There are significant differences between the ß-plane system and the spherical system. In the temperature field the variations range is from 5% to 50%. The

results of two systems are, however qualitatively the same.

References

1- Shankar, D., Vinayachandran P. N., and Unnikrishnan A. S., (2002), *The monsoon currents in the north Indian Ocean*. Progress in Oceanography, 52, 63–120.

2- Schott, FA, McCreary JP. (2001), *The Monsoon Circulation of the Indian Ocean*, Journal of Progress in Oceanography, 51(1), 1-123.

3- Shankar, D., Vinayachandran, P. N., and Unnikrishnan, A. S., (2002), *The monsoon currents in the north Indian Ocean*, Journal of Progress Oceanography, 52, 63–120.

4- Schott, FA, Xie SP, McCreary JP. (2009), *Indian Ocean Circulation and Climate Variability*. Reviews of Geophysics., 47(1), 1-46.

5- Muni Krishna K., Guiting Song, Dennis Jack and Manjunatha BR., (2014), *Tropical Indian Ocean Surface and Subsurface Temperature Fluctuations in a Climate Change Scenario*, Journal of Geology and Geophysics, 3(3), 1-17.

6- Kumar, M., (2011), *Methods for solving singular perturbation problems arising in science and engineering*, Journal of Mathematical and Computer Modelling, 54(1), 556–575.

7- Weinhart T., Singh, A., Thornton, A.R., (2010), *Perturbation Theory and Stability Analysis*, University of twente, 1-22.

8- Reason, Ch., (2011), *Circulation of the Indian Ocean and its climate variability with their impacts on northern Madagascar rainfall*, African Institute for Mathematical Sciences (AIMS).

9- bram, N. J., Gagan, M. K., Cole J. E., Hantoro, W. S., and Mudelsee, M., (2008), *Recent intensification of tropical climate variability in the Indian Ocean*, Journal of Geoscience, 1, 849–853.

10- Annamalai, H., and Murtugudde, R., (2004), *Role of the Indian Ocean in regional climate variability*, *in Earth's Climate: The Ocean-Atmosphere Interaction*, Journal of Geophysics, 147, 213–246.

11- Veronis, G. (1976), *Model of world ocean circulation, partII, Thermally driven, two layer,* Journal of marine research, 34, 199-216.

12- Welander, P. (1971), *Some exact solution to the equation describing an ideal fluid thermocline*, Journal of marine research, 22, 60-68.